Biochemistry and Biophysics Reports 10 (2017) 215–223

Contents lists available at ScienceDirect

Biochemistry and Biophysics Reports

journal homepage: www.elsevier.com/locate/bbrep

Structure, organization and tissue expression of the pig *SLC13A1* and *SLC13A4* sulfate transporter genes

Samuel K. Barnes[a], Yvonne A. Eiby[b], Soohyun Lee[a], Barbara E. Lingwood[b], Paul A. Dawson[a,*]

[a] Mater Research Institute, The University of Queensland, Woolloongabba, Queensland, Australia
[b] UQ Centre for Clinical Research, The University of Queensland, Brisbane, Queensland, Australia

ARTICLE INFO

Keywords:
Sulfate
Sus scrofa
Pig
Gene
Transporter
Placenta
Kidney

ABSTRACT

Sulfate is an obligate nutrient for fetal growth and development. In mice, the renal Slc13a1 sulfate transporter maintains high maternal circulating levels of sulfate in pregnancy, and the placental Slc13a4 sulfate transporter mediates sulfate supply to the fetus. Both of these genes have been linked to severe embryonal defects and fetal loss in mice. However, the clinical significance of *SLC13A1* and *SLC13A4* in human gestation is unknown. One approach towards understanding the potential involvement of these genes in human fetal pathologies is to use an animal model, such as the pig, which mimics the developmental trajectory of the human fetus more closely than the previously studied mouse models. In this study, we determined the tissue distribution of pig *SLC13A1* and *SLC13A4* mRNA, and compared the gene, cDNA and protein sequences of the pig, human and mouse homologues. Pig *SLC13A1* mRNA was expressed in the ileum and kidney, whereas pig *SLC13A4* mRNA was expressed in the placenta, choroid plexus and eye, which is similar to the tissue distribution in human and mouse. The pig *SLC13A1* gene contains 15 exons spread over 76 kb on chromosome 8, and encodes a protein of 594 amino acids that shares 90% and 85% identity with the human and mouse homologues, respectively. The pig *SLC13A4* gene is located approximately 11 Mb from *SLC13A1* on chromosome 8, and contains 16 exons spanning approximately 70 kb. The pig SLC13A4 protein contains 626 amino acids that share 91% and 90% identity with human and mouse homologues, respectively. The 5'-flanking region of *SLC13A1* contains several putative transcription factor binding sites, including GATA-1, GATA-3, Oct1 and TATA-box consensus sequences, which are conserved in the homologous human and mouse sequences. The 5'-flanking sequence of *SLC13A4* contains multiple putative transcription factor consensus sites, including GATA-1, TATA-box and Vitamin D responsive elements. This is the first report to define the tissue distribution of pig *SLC13A1* and *SLC13A4* mRNAs, and compare the gene, cDNA, 5'-flanking region and protein sequences to human and mouse.

1. Introduction

Sulfate is an important nutrient for numerous cellular and metabolic processes in human physiology [1]. Sulfate conjugation (sulfonation) to steroids and thyroid hormone leads to their inactivation by preventing their binding to receptors [2]. Sulfonation also plays an important role in the detoxification and urinary elimination of xenobiotics and some pharmacological agents [3,4]. In addition, the sulfate content of proteoglycans, such as heparan sulfate and chondroitin sulfate, is important for sequestering growth factors (e.g. VEGF) which contributes to regulating tissue growth and development [5,6]. Importantly, sufficient circulating levels of sulfate need to be maintained for sulfonation reactions to function effectively and to achieve the required biological balance of sulfonated to unconjugated substrates [7].

In humans and mice, inorganic sulfate is absorbed in the ileum and then maintained at abundant levels in circulation (human 0.3 mmol/L, mice 1.0 mmol/L) by the kidneys [8]. The solute linked carrier 13A1 (SLC13A1) sulfate transporter is expressed in the ileum and kidney where it mediates sulfate absorption and reabsorption, respectively [9]. During mouse pregnancy, increased *Slc13a1* mRNA expression in the kidney leads to increased maternal plasma sulfate levels that peak (2-fold increase) in third trimester when fetal growth and sulfate demands are high [10]. In human gestation, maternal plasma sulfate level also increases approximately 2-fold, suggesting that the physiological requirement for high circulating sulfate level in pregnancy is conserved across species [11]. A related sulfate transporter, SLC13A4, is expressed in the placenta where it mediates sulfate transfer to the developing fetus [10,12]. The physiological importance of maintaining high maternal plasma sulfate levels via SLC13A1, as well as placental sulfate transfer via SLC13A4, has been highlighted with findings of late-

* Corresponding author.
E-mail address: paul.dawson@mater.uq.edu.au (P.A. Dawson).

http://dx.doi.org/10.1016/j.bbrep.2017.04.005
Received 8 November 2016; Received in revised form 27 February 2017; Accepted 12 April 2017
Available online 13 April 2017

gestational fetal demise in *Slc13a1* and *Slc13a4* knockout mice [13–15].

The lethal consequence of targeted *Slc13a1* and *Slc13a4* disruption on mouse development has potential clinical relevance to fetal development in human gestation. Both genes are highly conserved (> 80% identity) and have similar tissue expression patterns in mice and humans [16,17]. In addition, loss-of-function mutations in human *SLC13A1* lead to renal sulfate wasting and reduced plasma sulfate levels [18,19], as found in the *Slc13a1* null mouse [13]. Over the past decade, several studies on the *Slc13a1* and *Slc13a4* null mice have provided valuable insights into the roles of these genes, particularly their obligate requirement for supplying sulfate from mother to fetus [13–15]. However, the importance of sulfate in human pregnancy is underappreciated and is not routinely measured in clinical settings [9]. In addition, dietary sulfate intake during pregnancy is not usually considered, despite evidence that diet can impact on circulating sulfate levels and sulfonation capacity [8]. Accordingly, further studies are warranted to investigate the potential pathogenetic involvement of *SLC13A1* and *SLC13A4* in human gestation, as well as the consequences of reduced sulfate levels in mother and child.

One approach towards investigating the potential clinical relevance of reduced sulfate availability to the fetus, as a consequence of disrupted *SLC13A1* or *SLC13A4* function, is to use a preclinical animal model such as the pig that mimics certain aspects of human gestation more closely than the mouse models [13,15,20]. For example, the pig fetus has a similar size, organ architecture and tissue developmental trajectory when compared to the human fetus, and its gestational period (115 days) is closer to the length of human gestation (259–280 days) than that of the mouse (19–21 days) [21,22]. However, before we consider any studies to investigate sulfate biology in the pig fetus, we first need to determine whether the tissue expression profiles and gene structures of pig *SLC13A1* and *SLC13A4* are conserved with human and mouse homologues.

In this study, we report the gene, cDNA and protein sequences of pig *SLC13A1* and *SLC13A4*, and compare those to the human and mouse homologues. Our study also reports the tissue distribution of *SLC13A1* and *SLC13A4* mRNA expression in several pig tissues, as well as putative response elements in the 5'-flanking regions of these genes.

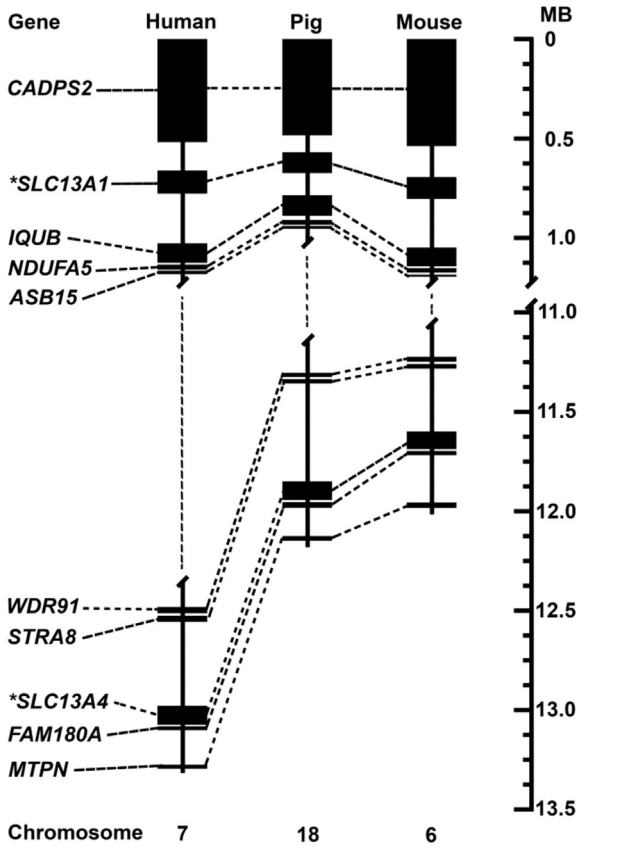

Fig. 1. Pig *SLC13A1* and *SLC13A4* chromosomal localization. *Comparative locations of *SLC13A1* and *SLC13A4* on pig chromosome 18 (assembly Sscrofa10.2, NC_010460.3), human chromosome 7 (assembly GRCh38.p7, NC_000007.14) and mouse chromosome 6 (assembly GRCm38.p4, NC_000072.6). Also shown are those genes surrounding *SLC13A1* (*CADPS2*, *IQUB*, *NDUFA5*, *ASB15*) and *SLC13A4* (*WDR91*, *STRA8*, *FAM180A*, *MTPN*).

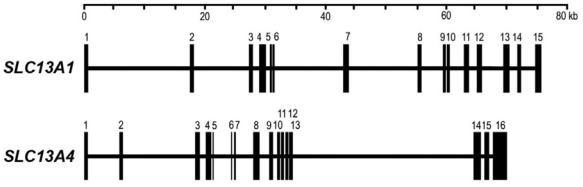

Fig. 2. Pig *SLC13A1* and *SLC13A4* gene structures. Exon-intron organization showing exons (vertical lines) and introns (horizontal lines) spread over approximately 76 kb (*SLC13A1*) and 70 kb (*SLC13A4*).

2. Materials and methods

2.1. Gene, cDNA and protein sequences

We undertook a search of the NCBI Gene, Nucleotide and Protein databases (https://www.ncbi.nlm.nih.gov/) using the terms "*SLC13A1*" or "*SLC13A4*", and "*Sus scrofa*" within the date range of 1 April 2016 to 1 May 2016. To determine the nucleotide sequences of intron/exon junctions, transcription initiation start sites, and the 5'-flanking regions, we aligned the curated pig *SLC13A1* (XM_013985680.1) and *SLC13A4* (XM_003134643.3) mRNA sequences with pig genome sequence (NC_010460.3). Putative transcription factor binding motifs within the first 1000 nucleotides of the 5'-flanking regions of pig *SLC13A1* and *SLC13A4* were identified using MatInspector software [23], and compared to the published *SLC13A1* and *SLC13A4* gene promoter findings for human and mouse [16,24–26]. Amino acid sequences of pig SLC13A1 (XP_013841134.1) and SLC13A4 (XP_003134691.1) were aligned to human and mouse homologue proteins using ClustalW software [27]. Potential transmembrane domains (TMDs), protein kinase A, protein kinase C, casein kinase II and N-glycosylation sites were identified based on conserved amino acid sequences in the homologous proteins of human and mouse [16,24,26,28].

2.2. Animals, tissues and RNA isolation

Large White/Landrace cross sows were fed water ad libitum and standard pig feeds: Riverina Pig Grower for non-pregnant sows, and Riverina Pig Breeder for pregnant sows. The levels of total protein (16.00%) and methionine (RPG 0.22%; RPB 0.20%), as well as the sulfate salts of zinc (120 mg/kg), manganese (45 mg/kg), iron (100 mg/kg) and copper (10 mg/kg) were similar between both diets (Riverina Stock Feeds, Australia). Approximate body masses of non-pregnant and pregnant sows were 80 and 250 kg, respectively. Three non-pregnant sows were selected at 16 weeks of age to be euthanized for collection of kidney, heart, skin, ileum, lung, spleen, muscle, liver, ovary, uterus, eye, and dissected brain regions (frontal lobe and choroid plexus). Two additional pregnant sows at approximately 2 years of age were selected for collection of placental tissue at 98 days gestation (term = 115 days). All procedures were approved by the University of Queensland Animal Ethics Committee. Total RNA was isolated from each tissue using TRIzol® reagent according to the manufacturer's protocol (Invitrogen). First strand cDNA was generated using 2 μg of DNase I treated RNA and a Transcriptor cDNA Synthesis Kit (Roche).

Table 1
Exon-intron organization of pig *SLC13A1*.

Intron No.	Phase	5' splice donor[a]	Intron (bp)[b]	3' splice acceptor[a]	Exon No.	Exon (bp)
1	0	ACCAAG/gtaagtgag	17,994	tccgtccag/GAAGCA	1	134
2	0	AAGGAG/gtaagtgag	9718	taatttcag/GTGGCA	2	129
3	1	AGCATG/gtaagtact	2444	tcatttcag/GCTGAC	3	137
4	2	CTGATG/atatgacat	582	tgttttcag/AAAGTG	4	188
5	1	TGCAGG/gtaaagaat	81	atttttcag/ATACAG	5	58
6	0	GAAAAG/gtacattaa	12,780	gttgaacag/AACTCA	6	49
7	1	CAATAT/gtaagtaca	11,082	ttcacacag/GCGCTA	7	152
8	1	ATTCAA/gtgagtaca	4328	tctttttag/TTTTAA	8	120
9	1	AATAAG/gtaagatac	439	ttccaacag/GTATCA	9	99
10	1	TTCGCA/gtaagcgtt	3289	tcttttcag/GTATCC	10	102
11	2	AAACTG/gttgagtat	2030	gttttgtag/TTGCTT	11	107
12	0	TGTGAG/gtaatattc	4689	ttttttag/GAGTCA	12	110
13	0	CCATTG/gtgagtatc	1489	tccaacaag/GCTGAA	13	162
14	0	GACATG/gtgagtgag	2261	gtattcaag/GTTAAA	14	138
					15	166

[a] Exon sequences are indicated by uppercase letter and intron sequences by lowercase letters
[b] Intronic sequences were determined from the alignment of pig genomic DNA (NC_010460.3) and *SLC13A1* cDNA (XM_013985680.1) sequences.

Table 2
Exon-intron organization of pig *SLC13A4*.

Intron No.	Phase	5' splice donor[a]	Intron (bp)[b]	3' splice acceptor[a]	Exon No.	Exon (bp)
1	0	AGCAGC/gtgagtacc	6023	cccttccag/GAGGCT	1	123
2	0	AACGAG/gttagacca	13,466	cctctgcag/GTGGCG	2	129
3	1	AGGCAT/gtaagtcac	1811	cccttccag/GCTGCT	3	137
4	2	TCATCA/gtacagttt	450	ctactgtag/GTCTCA	4	173
5	1	TGAAGA/gtgagtatg	2490	ttcctgcag/CACGTC	5	55
6	0	AACAAG/gtatggcct	880	tcccgacag/AACCTG	6	40
7	0	CCCCAG/gtaatgcaa	2247	ctttgctag/GAAAAG	7	78
8	1	CAACAA/gtaagccac	2701	tccctccag/CCAGTA	8	185
9	1	CTGCAA/gtgagtccc	1049	ccttctcag/TTTTAA	9	120
10	1	CGTTAG/gtgggaatc	320	attttatag/TTACCC	10	102
11	1	TGAAAA/gtaagtaat	721	ctttgccag/GAAGGG	11	102
12	2	ATGATG/gtgagagga	222	gtgatccag/GGGAGG	12	98
13	0	AGCAAG/gtaaccctt	32,108	tccctgcag/ACCTCT	13	125
14	0	AGCTTG/gtgagtaga	1345	ctcttctag/TCGGAG	14	162
15	0	GATATG/gtgagtcac	2162	gtcccgcag/GTGAAA	15	138
					16	1198

[a] Exon sequences are indicated by uppercase letter and intron sequences by lowercase letters.
[b] Intronic sequences were determined from the alignment of pig genomic DNA (NC_010460.3) and *SLC13A4* cDNA (XM_003134643.3) sequences.

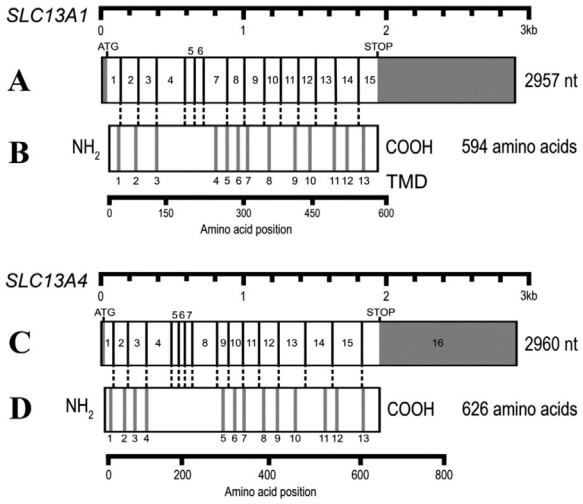

Fig. 3. Pig *SLC13A1* and *SLC13A4* cDNA structures. (A) Schematic showing exons 1–15 (boxes) and protein coding sequences (white portions) for *SLC13A1* spread over 2957 nucleotides. (B) The predicted 13 transmembrane spanning domains (grey bands) of SLC13A1 protein aligned with *SLC13A1* cDNA (dashed lines). (C) Schematic showing exons 1–16 (boxes) and protein coding sequences (white portions) spread over 2960 nucleotides. (D) The predicted 13 transmembrane spanning domains (grey bands) of SLC13A4 protein aligned with *SLC13A4* cDNA (dashed lines).

2.3. PCR analyses to determine tissue distribution of SLC13A1 and SLC13A4 mRNA

Primer 5'-TTGCCTGGACTAATGTTCCC-3' and reverse primer 5'-TGCCTGATATTTTTCCTGCC-3' were used to amplify 463 bp *SLC13A1* cDNA fragments. Primer 5'-GGCCTTCTCCGAGCCAGG-3' and reverse primer 5'-CTGACCAGCTCCTGCAGCAC-3' were used to amplify 400 bp *SLC13A4* cDNA fragments. Control 470 bp β-actin cDNA fragments were amplified using forward 5'- GGACCTGACCGACTACCTCA-3' and reverse 5'-ACACGGAGTACTTGCGCTCT-3' primer sequences. Each PCR included 200 nM forward and reverse primers, first strand cDNA (equivalent to 0.2 µg RNA), 1.6 mM dNTPs and 1 Unit DNA polymerase (Scientifix). The thermal cycling protocol was: 35 cycles of 95 °C for 30 s, 55 °C for 30 s, and 72 °C for 2 min; followed by 72 °C for 5 min. PCR-amplified DNA was size-fractioned in a 1.5% agarose gel and then visualised using SYBR® safe DNA stain (Invitrogen) under UV light.

3. Results and discussion

In this study, we report the pig *SLC13A1* and *SLC13A4* gene, cDNA, 5'-flanking region and protein sequences, as well as the tissue distribution of *SLC13A1* and *SLC13A4* mRNA, and compare those to the previously published findings for the human and mouse homologues. Our findings show that the structure and tissue expression of both *SLC13A1* and *SLC13A4* are conserved between pig, human and mouse,

which suggests conserved physiological roles for these genes in maintaining sulfate homeostasis in the pig.

The pig *SLC13A1* and *SLC13A4* genes are located on chromosome 18 which maps to regions of conserved synteny with homologues on human chromosome 7 and mouse chromosome 6 (Fig. 1). The intergenic region between pig *SLC13A1* and *SLC13A4* spans approximately 11 Mb and contains more than 60 genes, including *IQUB*, *NDUFA5*, *ASB15*, *WDR91* and *STRA8*, which are conserved within the corresponding 12 Mb human and 11 Mb mouse regions. Co-localization of *SLC13A1* and *SLC13A4* on the same chromosome in pig, human and mice, suggests that these 2 related genes may be derived from a gene duplication event through evolution. Indeed, pig *SLC13A1* and *SLC13A4* share similar genomic arrangements, with exons 2, 3, 8, 10, 13 and 14 of *SLC13A1* sharing the identical number of nucleotides to exons 2, 3, 9, 11, 14 and 15 of *SLC13A4* (Fig. 2, Tables 1 and 2). In addition, the arrangement of pig *SLC13A1* and *SLC13A4* are similar to those reported for the human and mouse homologues [16,17]. Pig *SLC13A1* contains 15 exons spread over 76 kb, compared to human *SLC13A1* (15 exons, 87 kb) and mouse *Slc13a1* (15 exons, 76 kb) [24,28]. Pig *SLC13A4* contains 16 exons spanning approximately 70 kb, compared to human *SLC13A4* (16 exons, 47.0 kb) and mouse *Slc13a4* (16 exons, 40.1 kb) [16,26]. The overall larger size of pig *SLC13A4* when compared to human and mouse, is mostly attributed to intron 13 (32Kb) in pig *SLC13A4*, which is markedly larger than intron 13 in human *SLC13A4* (5.5 kb) and mouse *Slc13a4* (3.1Kb) [16,26].

The pig *SLC13A1* cDNA is 2957 nucleotides, with 38 bases of 5'-UTR, 1782 bases of coding region and 1134 bases of 3'-UTR (Fig. 3A). Pig *SLC13A4* cDNA is 2960 nucleotides, with 24 bases of 5'-UTR, 1877 bases of coding region and 1055 bases of 3'-UTR. Alignment of genomic and cDNA sequences for both pig *SLC13A1* and *SLC13A4*, showed the

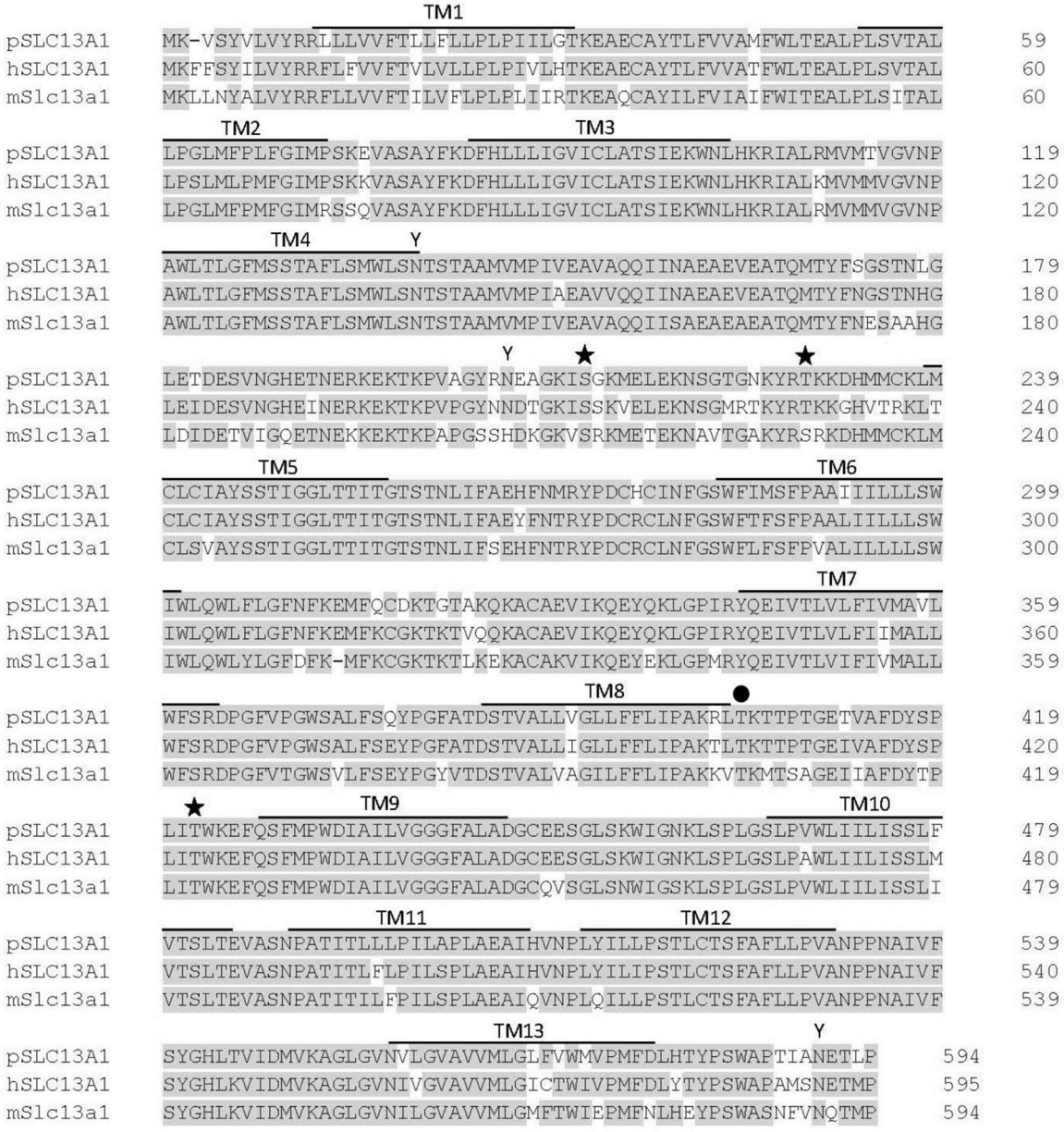

Fig. 4. Pig SLC13A1 amino acid sequence aligned with human and mouse sequences. Alignments were generated using the Clustal W program [27]. Identical amino acids are highlighted in grey. Putative transmembrane domains (TM1 to TM13) are indicated by bold face lines. Potential phosphorylation (• protein kinase A; ★ protein kinase C) and N-glycosylation (Y) sites are indicated.

nucleotide sequences at the intron-exon boundaries to conform to the GT/AG rule for intron donor and acceptor sites (Tables 1 and 2). Codon phase is mainly 0 or 1 for pig *SLC13A1* and *SLC13A4*, which differs to the human and mouse homologues that have mostly 0 or 2 codon phase [16,24,26,28]. The biological relevance of this finding is unknown but may be the result of evolutionary divergence of pig from human and mouse approximately 97 million years ago [29]. The translation initiation site is present in exon 1 of pig *SLC13A1* and *SLC13A4*, and a TGA stop codon is situated in exons 15 and 16 of *SLC13A1* and *SLC13A4*, respectively (Fig. 3).

The pig SLC13A1 protein contains 594 amino acids and shares 90% and 85% identity with human SLC13A1 and mouse Slc13a1, respectively (Fig. 4). Alignment of SLC13A4 proteins shows the pig amino acid sequence of 626 amino acids to have 91% and 90% identity with human and mouse (Fig. 5). The 13 predicted transmembrane domains (TMDs) in pig SLC13A1 and SLC13A4 share high amino acid identity (range 80–100%) with the human and mouse homologues (Fig. 4 and 5). Comparison of the TMDs in pig SLC13A1 and SLC13A4 with exon location shows that each TMD is encoded by a separate exon, with the exception of TMDs 5 and 6 in SLC13A1 which are encoded by exon 8, and TMDs 8 and 9 in SLC13A4 which are encoded by exon 12 (Fig. 3). These alignments also show that the TMDs are in close proximity to

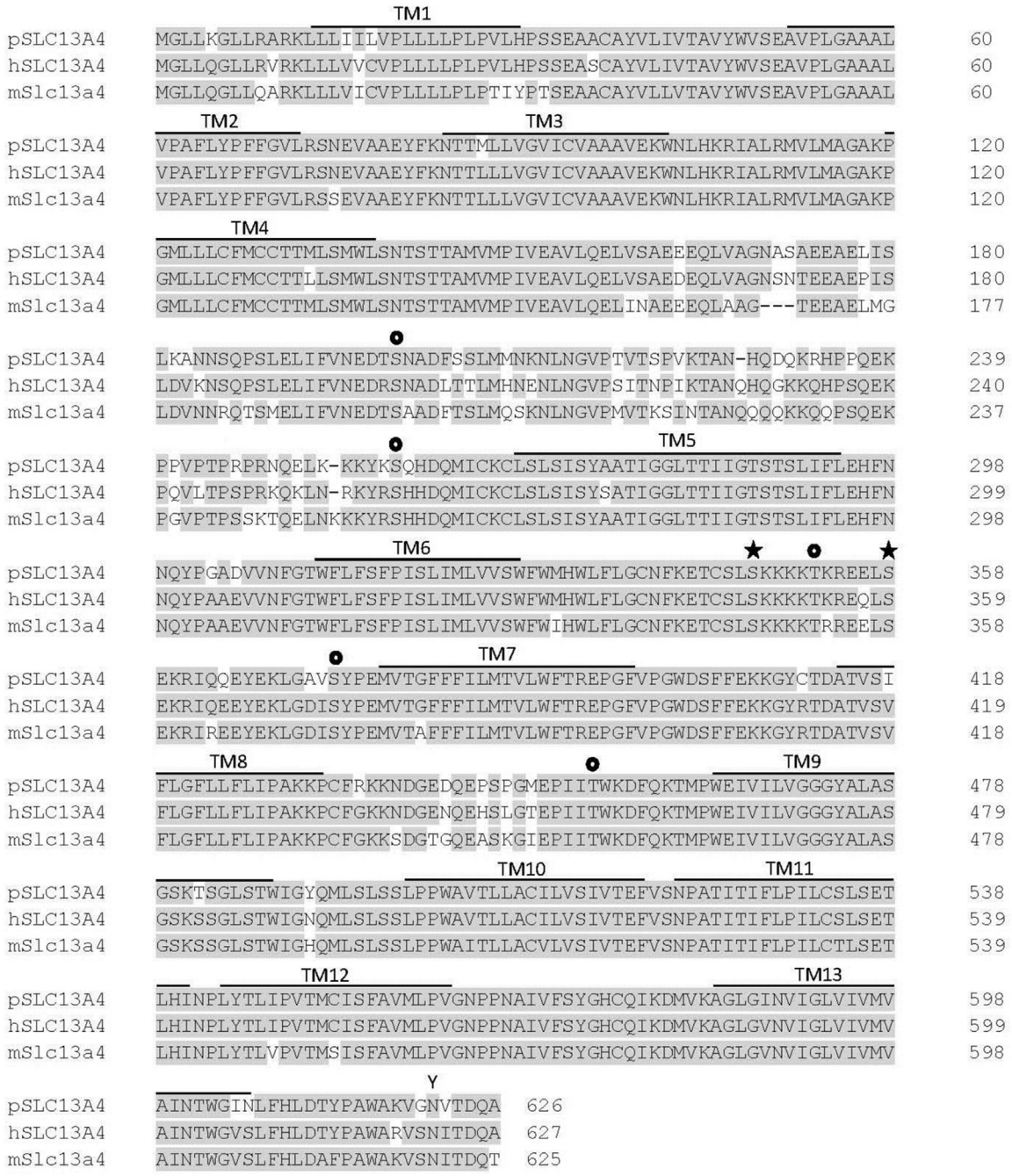

Fig. 5. Pig SLC13A4 amino acid sequence aligned with human and mouse sequences. Alignments were generated using the Clustal W program [27]. Identical amino acids are highlighted in grey. Putative transmembrane domains (TM1 to TM13) are indicated by boldface lines. Potential phosphorylation (★ protein kinase C; ● casein kinase II) and N-glycosylation (Y) sites are indicated.

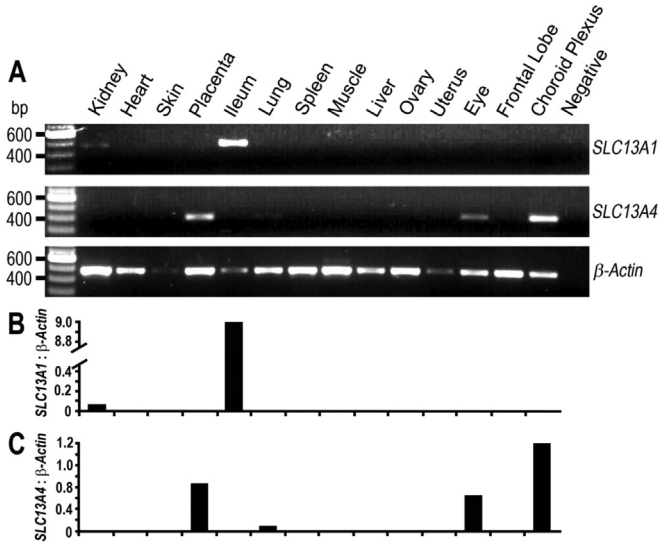

Fig. 6. Tissue distribution of pig *SLC13A1* and *SLC13A4* mRNA. (A) RT-PCR amplification of 463 bp *SLC13A1*, 400 bp *SLC13A4* and 470 bp β-*actin* cDNA fragments. (B-C) Densitometric analysis of the *SLC13A1*, *SLC13A4* and β-*actin* PCR products in (A). Placental tissue was derived from 2-year old pregnant sows, whereas all other tissues were from 16 wk old non-pregnant sows. Data are representative of three separate experiments.

exon boundaries, suggesting that splicing more frequently occurs near those nucleotide sequences that encode the junctions of hydrophobic/hydrophilic amino acids. A similar observation has been made for other proteins with TMDs expressed on the plasma membrane, including the SLC2A1, SLC2A2 and SLC2A4 glucose transporters [30].

The pig SLC13A1 and SLC13A4 proteins also contain consensus sequences for potential post-translational modifications (Fig. 4 and 5): protein kinase C sites in SLC13A1 (Ser^{212}, Thr^{223}, Thr^{422}) and SLC13A4 (Ser^{347}, Ser^{358}); 1 protein kinase A site in SLC13A1 (Thr^{404}); 5 casein kinase II in SLC13A4 (Ser^{200}, Ser^{258}, Thr^{352}, Ser^{373}, Thr^{454}), and *N*-glycosylation sites in SLC13A1 (Asn^{139}, Asn^{206}, Asn^{590}) and SLC13A4 (Asn^{621}). All of these amino acids are identical with the human and mouse homologues, suggesting a conserved role for phosphorylation and glycosylation in regulating the function or expression of SLC13A1 and SLC13A4 on the plasma membrane. However, based on the 13 TMD topology model for SLC13A1, the consensus sequences for *N*-glycosylation at positions Asn^{139} and Asn^{206} are predicted to be intracellular and therefore are unlikely to be glycosylated. This is supported by a previous study showing *N*-glycosylation to only occur on Asn^{591} in human SLC13A1, which corresponds to Asn^{590} in pig SLC13A1 [31].

Pig *SLC13A1* mRNA was detected in ileum and kidney, whereas pig *SLC13A4* mRNA was detected in the placenta, choroid plexus and eye (Fig. 6), which is similar with the tissue distribution of the human and mouse homologues [16,17,26]. SLC13A1 is localized to the apical membrane of epithelial cells in the ileum and renal proximal tubule of mice, where it mediates sulfate absorption and reabsorption, respectively [13]. Using RT-PCR, our findings show abundant levels of *SLC13A1* mRNA in the ileum, suggesting a high requirement for SLC13A1 in mediating absorption of sulfate in the pig ileum. Previous studies showed abundant *Slc13a1* mRNA in the mouse ileum and kidney [24], whereas *SLC13A1* mRNA was exclusively detected in the human kidney and not in the small intestine [28]. However, a recent search of the NCBI database (24 February 2017, www.ncbi.nlm.nih.gov/est/) using the search terms “SLC13A1” and “Homo sapiens” revealed expression of *SLC13A1* mRNA in human intestine at approximately 7% of kidney *SLC13A1* mRNA levels. Our findings of low *SLC13A1* mRNA levels in the pig kidney, compared to levels in the ileum (Fig. 6A,B), are not consistent with the ratio in kidney and ileum of human and mouse. Identifying the relative contributions of renal reabsorption and ileal absorption to maintaining circulating sulfate levels in the pig will be the next phase of our research. The role of SLC13A4 in the eye and choroid plexus is unknown but is most likely to be mediating sulfate supply to the eye and brain for sulfonation of proteoglycans, such as heparan sulfate and chondroitin sulfate which play important roles in maintaining the structure and function of the eye and brain [9,32,33]. In addition, sulfonation of neurotransmitters and thyroid hormone in the brain contribute to neurological function and neurodevelopment, suggesting a potential role for SLC13A4 in maintaining sulfate homeostasis in the brain [2,34]. Our finding of abundant *SLC13A4* mRNA in the pig placenta (Fig. 6A,C) is relevant to recent studies showing the critical role of Slc13a4 in supplying sulfate to the developing mouse fetus [15]. Targeted disruption of placental *Slc13a1* in mice leads to developmental defects from embryonal day E12.5, and fetal death prior to birth around E18.5. SLC13A4 is expressed in the syncytiotrophoblast layer of the human and mouse placenta [10,12], where it plays a non-redundant role of supplying sulfate from the maternal circulation to the mouse fetus [15]. Whilst the epitheliochorial architecture of the pig placenta is structurally different to human and mouse hemochorial placentation, it is likely that pig SLC13A4 contributes to fetal sulfate supply based on its abundant mRNA expression in the placenta.

We acknowledge the age difference between the non-pregnant (16 wk) and pregnant (2 yr) sows used in this study, and the potential different sulfate demands in these two groups, which is relevant when considering *SLC13A1* and *SLC13A4* mRNA expression levels. Studies in rodents show that renal *Slc13a1* mRNA increases approximately 2-fold during mouse pregnancy [10], and decreases in 22–23 month old rats beyond reproductive age [35]. Whilst placental *Slc13a4* mRNA increases during rodent gestation [10], the impact of age and pregnancy on *Slc13a4* expression in non-placental tissues, including brain, eye and lung, has not been reported. The impact of diet is also an important consideration for sulfate homeostasis and sulfate transporter gene expression [8]. In particular, previous studies have shown that decreased methionine intake can alter sulfate homeostasis in pigs and rats [36,37]. However, the two diets used in the present study for pregnant and non-pregnant pigs, contained similar methionine levels and thereby are unlikely to have impacted on *SLC13A1* and *SLC13A4* mRNA levels. While this study reports the tissue distribution of *SLC13A1* and *SLC13A4* mRNA expression, further studies are warranted to investigate the consequences of ageing, pregnancy status and diet on *SLC13A1* and *SLC13A4* expression levels in the pig, which are relevant to maintaining sulfate homeostasis in human gestation.

The 5’-flanking region of the pig *SLC13A1* gene contains several putative transcription factor binding (TFB) sites (Fig. 7A), including GATA1 (at −798 nt, and at −242 nt), Oct-1 (at −798 nt, −136 nt and −131 nt), HNF4 (at −655 nt and −181 nt), GMEB2 (at −547 nt), GATA3 (at −17 nt) and TATA-boxes VTATA (at −113 nt) and TATA (at −12). Whilst these consensus sites share similar locations in the 5’-flanking regions of the homologous pig, human and mouse sequences (Fig. 7B), their involvement in the transcriptional regulation of *SLC13A1* mRNA is yet to be determined. Analysis of the pig *SLC13A4* 5’-flanking region identified numerous putative TFB sites (Fig. 8A), including SREBP (at −978 nt), GATA1 (at −867 nt), AP-1 (at −860 nt), HNF4 (at −725 nt), AP-2 (at −693 nt), FAST1 (at −525 nt), NF1 (at −451 nt), EN-1 (at −394 nt), CEBPB (at −324 nt), STAT5A (at −101 nt), CCAAT box (at −839 nt), a GC SBE box (at −814 nt), IR2 NGRE (at −11 nt), a vertebrate conserved TATA-box (VTATA at −389 nt) and a Vitamin D motif (VDR RXR; at – 22 nt). Remarkably, these consensus sites are not conserved with sequences in the 5’-flanking regions of human *SLC13A4* and mouse *Slc13a4* (Fig. 8). This observation may be relevant when considering the epitheliochorial structure of

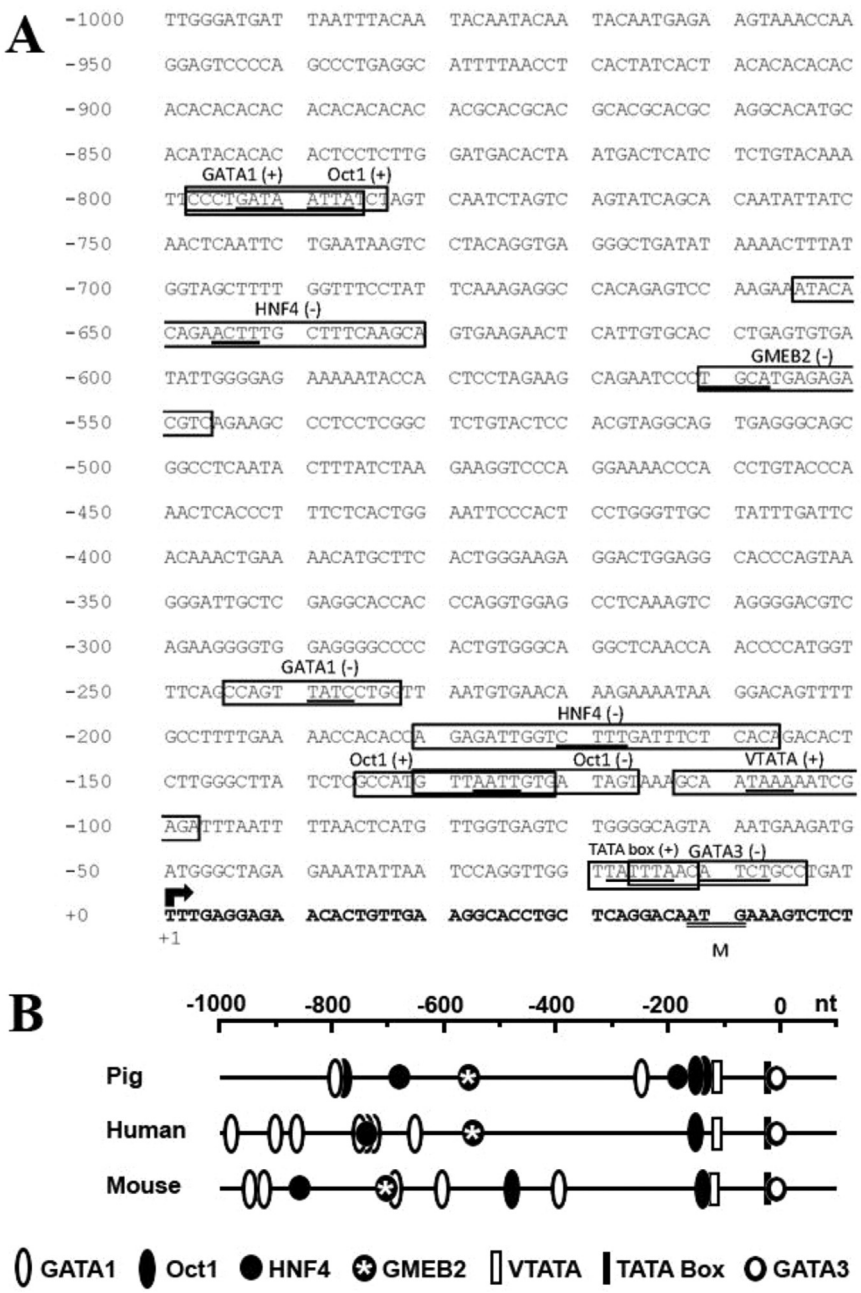

Fig. 7. Location of putative transcription factor binding motifs in the pig *SLC13A1* 5'-flanking region. (A) Nucleotide sequence of the predicted *SLC13A1* 5'-flanking region (from −1000 to +50) is shown. Position +1 (arrow) denotes the putative transcription initiation site. The translation initiation ATG codon is double underlined. Boldface letters indicate the 5'-region of exon 1. A vertebrate conserved TATA box as well as putative transcription factor binding motifs are boxed, with core sequences underlined. Potential binding motifs were identified using MatInspector [23] with parameters of core > 0.9 and matrix > 0.8 similarities. GATA1, GATA binding factor 1; Oct-1, octamer factor 1; HNF4, hepatic nuclear factor 4; GMEB2, glucocorticoid modulatory element binding protein 2; and GATA3, GATA binding factor 3. (B) Relative locations of each transcription-factor binding site were compared to those previously reported in the 5'-flanking region of human *SLC13A1* and mouse *Slc13a1* [24,25].

the pig placenta, versus the different architecture of human and mouse hemochorial placentation. In addition, comparison of the pig *SLC13A1* and *SLC13A4* 5'-flanking regions shows a very different profile of the putative TFB sites (Fig. 7B versus Fig. 8B), which could contribute to the tissue specific expression profiles of these 2 genes (Fig. 6). Interestingly, a slightly higher AT-content was observed in the 5'-flanking regions of the pig *SLC13A1* (55% AT versus 45% GC) and *SLC13A4* (51% AT versus 49% GC). This may be relevant to the higher AT-content in the promoters of genes that are regulated during development and have a specific tissue distribution [38], as is the case for *SLC13A1* and *SLC13A4*.

In summary, this is the first report to characterise the tissue distribution of pig *SLC13A1* and *SLC13A4* mRNA. We have also presented the gene and cDNA structures, protein sequences and putative TFB sites for both of these genes, and compared those sequences to the human and mouse homologues. The highly conserved sequences and tissue expression patterns of both genes in pig, human and mouse, indicates that the pig is most likely an appropriate model of sulfate regulation in human pregnancy. Overall, this information provides a resource for further investigating the role of *SLC13A1* and *SLC13A4* in maintaining sulfate homeostasis in pig gestation, which should lead to a more detailed understanding of sulfate physiology in maternal and child health.

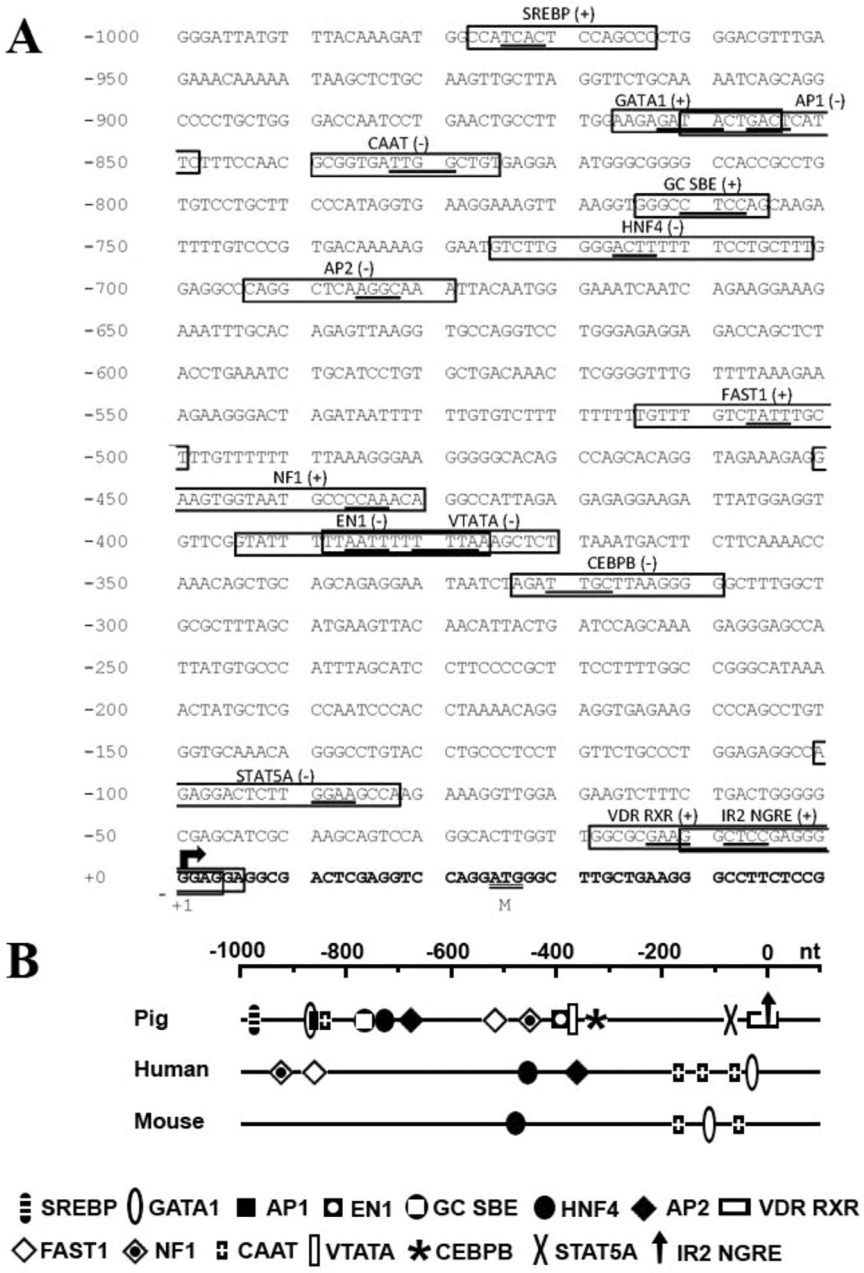

Fig. 8. Location of putative transcription factor binding motifs in the pig *SLC13A4* 5'-flanking region. (A) Nucleotide sequence of the predicted *SLC13A4* 5'-flanking region (from −1000 to +50) is shown. Position +1 (arrow) denotes the putative transcription initiation site. The translation initiation ATG codon is double underlined. Boldface letters indicate the 5'-region of exon 1. A vertebrate conserved TATA box, CAAT-box, Vitamin-D binding site (VDR RXR) and GC- (SBE binding site) as well as putative transcription factor binding motifs are boxed, with core sequences underlined. Potential binding motifs were identified using MatInspector [23] with parameters of core > 0.9 and matrix > 0.8 similarities. SREBP, sterol regulatory element binding protein; GATA1, GATA binding factor 1; AP-1, associated protein 1; HNF4, hepatic nuclear factor 4; AP-2, associated protein 2; FAST1, FAST1 SMAD interacting protein; NF1, nuclear factor 1; EN1, homeobox protein engrailed; CEBPB, CCAAT/ enhancer binding protein beta; and STAT5A, signal transducer and activator of transcription factor 5. (B) Relative locations of each transcription-factor binding site were compared to those previously reported in the 5'-flanking region of human *SLC13A4* and mouse *Slc13a4* [16,26].

Acknowledgements

This work was supported by Mater Research, a Mater Clinical Research Seeding Grant, the Queensland Perinatal Consortium (QPaCt) and a Mater Foundation Research Fellowship to P.A.D.

Appendix A. Transparency document

Transparency document associated with this article can be found in the online version at http://dx.doi.org/10.1016/j.bbrep.2017.04.005.

References

[1] P.A. Dawson, Role of sulphate in development, Reproduction 146 (2013) R81–R89.
[2] P.A. Dawson, The biological roles of steroid sulfonation, in: S.M. Ostojic (Ed.), Steroids - From Physiology to Clinical Medicine, Intech, Rijeka, 2012, pp. 45–64.
[3] M.W. Coughtrie, K.J. Bamforth, S. Sharp, A.L. Jones, E.B. Borthwick, E.V. Barker, R.C. Roberts, R. Hume, A. Burchell, Sulfation of endogenous compounds and xenobiotics–interactions and function in health and disease, Chem. Biol. Interact. 92 (1994) 247–256.
[4] S.D. Nelson, W.P. Gordon, Mammalian drug metabolism, J. Nat. Prod. 46 (1983) 71–78.
[5] H. Habuchi, O. Habuchi, K. Kimata, Sulfation pattern in glycosaminoglycan: does it have a code? Glycoconj. J. 21 (2004) 47–52.
[6] M. Klüppel, The roles of chondroitin-4-sulfotransferase-1 in development and disease, Prog. Mol. Biol. Transl. Sci. 93 (2010) 113–132.

[7] S. Lee, P.A. Dawson, A.K. Hewavitharana, P.N. Shaw, D. Markovich, Disruption of NaS1 sulfate transport function in mice leads to enhanced acetaminophen-induced hepatotoxicity, Hepatology 43 (2006) 1241–1247.
[8] P.A. Dawson, A. Elliott, F.G. Bowling, Sulphate in pregnancy, Nutrients 7 (2015) 1594–1606.
[9] P.A. Dawson, Sulfate in fetal development, Semin. Cell Dev. Biol. 22 (2011) 653–659.
[10] P.A. Dawson, J. Rakoczy, D.G. Simmons, Placental, renal, and ileal sulfate transporter gene expression in mouse gestation, Biol. Reprod. 87 (2012) 1–9.
[11] P.A. Dawson, S. Petersen, R. Rodwell, P. Johnson, K. Gibbons, A. McWhinney, F.G. Bowling, H.D. McIntyre, Reference intervals for plasma sulfate and urinary sulfate excretion in pregnancy, BMC Pregnancy Childbirth 15 (2015), http://dx.doi.org/10.1186/s12884-12015-10526-z.
[12] D.G. Simmons, J. Rakoczy, J. Jefferis, R. Lourie, H.D. McIntyre, P.A. Dawson, Human placental sulfate transporter mRNA profiling identifies abundant SLC13A4 in syncytiotrophoblasts and SLC26A2 in cytotrophoblasts, Placenta 34 (2013) 381–384.
[13] P.A. Dawson, L. Beck, D. Markovich, Hyposulfatemia, growth retardation, reduced fertility and seizures in mice lacking a functional NaS_i-1 gene, Proc. Natl. Acad. Sci. USA 100 (2003) 13704–13709.
[14] P.A. Dawson, P. Sim, D.G. Simmons, D. Markovich, Fetal loss and hyposulfataemia in pregnant NaS1 transporter null mice, J. Reprod. Dev. 57 (2011) 444–449.
[15] J. Rakoczy, Z. Zhang, F.G. Bowling, P.A. Dawson, D.G. Simmons, Loss of the sulfate transporter Slc13a4 in placenta causes severe fetal abnormalities and death in mice, Cell Res. 25 (2015) 1273–1276.
[16] P.A. Dawson, K.J. Pirlo, S.E. Steane, K. Kunzelmann, Y.J. Chien, D. Markovich, Molecular cloning and characterization of the mouse Na+ sulfate cotransporter gene (Slc13a4): structure and expression, Genes Genet. Syst. 81 (2006) 265–272.
[17] A. Lee, P.A. Dawson, D. Markovich, NaSi-1 and Sat-1: structure, function and transcriptional regulation of two genes encoding renal proximal tubular sulfate transporters, Int. J. Biochem. Cell Biol. 37 (2005) 1350–1356.
[18] F.G. Bowling, H.S. Heussler, A. McWhinney, P.A. Dawson, Plasma and urinary sulfate determination in a cohort with autism, Biochem. Genet. 51 (2012) 147–153.
[19] C.G. Tise, J.A. Perry, L.E. Anforth, M.A. Pavlovich, J.D. Backman, K.A. Ryan, J.P. Lewis, J.R. O'Connell, L.M. Yerges-Armstrong, A.R. Shuldiner, From genotype to phenotype: nonsense variants in SLC13A1 are associated with decreased serum sulfate and increased serum aminotransferases, Genes Genomes Genet. 6 (2016) 2909–2918.
[20] Y.A. Eiby, N.Y. Shrimpton, I.M. Wright, E.R. Lumbers, P.B. Colditz, G.J. Duncombe, B.E. Lingwood, Inotropes do not increase cardiac output or cerebral blood flow in preterm piglets, Pediatr. Res. (2016), http://dx.doi.org/10.1038/pr.2016.1156.
[21] S.A. Book, L.K. Bustad, The fetal and neonatal pig in biomedical research, J. Anim. Sci 38 (1974) 997–1002.
[22] Y.A. Eiby, L.L. Wright, V.P. Kalanjati, S.M. Miller, S.T. Bjorkman, H.L. Keates, E.R. Lumbers, P.B. Colditz, B.E. Lingwood, A pig model of the preterm neonate: anthropometric and physiological characteristics, PLoS One 8 (2013) e68763.
[23] K. Quandt, K. Frech, H. Karas, E. Wingender, T. Werner, MatInd and MatInspector - New fast and versatile tools for detection of consensus matches in nucleotide sequence data, Nucleic Acids Res. 23 (1995) 4878–4884.
[24] L. Beck, D. Markovich, The Mouse Na+-Sulfate Cotransporter Gene Nas1: cloning, tissue distribution, gene structure, chromosomal assignment, and transcriptional regulation by vitamin D, J. Biol. Chem. 275 (2000) 11880–11890.
[25] A. Lee, D. Markovich, Characterization of the human renal Na(+)-sulphate cotransporter gene (NAS1) promoter, Pflug. Arch. 448 (2004) 490–499.
[26] D. Markovich, R.R. Regeer, K. Kunzelmann, P.A. Dawson, Functional characterization and genomic organization of the human Na(+)-sulfate cotransporter hNaS2 gene (SLC13A4), Biochem. Biophys. Res. Commun. 326 (2005) 729–734.
[27] D.G. Higgins, A.J. Bleasby, R. Fuchs, CLUSTAL V: improved software for multiple sequence alignment, Comput. Appl. Biosci. 8 (1992) 189–191.
[28] A. Lee, L. Beck, D. Markovich, The human renal sodium sulfate cotransporter (SLC13A1; hNaSi-1) cDNA and Gene: organisation, chromosomal localization, and functional characterization, Genomics 70 (2000) 354–363.
[29] M.A. Groenen, A.L. Archibald, H. Uenishi, C.K. Tuggle, Y. Takeuchi, M.F. Rothschild, C. Rogel-Gaillard, C. Park, D. Milan, H.J. Megens, S. Li, D.M. Larkin, H. Kim, L.A. Frantz, M. Caccamo, H. Ahn, B.L. Aken, A. Anselmo, C. Anthon, L. Auvil, B. Badaoui, C.W. Beattie, S. Zhao, J. Rogers, C. Churcher, L.B. Schook, Analyses of pig genomes provide insight into porcine demography and evolution, Nature 491 (2012) 393–398.
[30] G.I. Bell, T. Kayano, J.B. Buse, C.F. Burant, J. Takeda, D. Lin, H. Fukumoto, S. Seino, Molecular biology of mammalian glucose transporters, Diabetes Care 13 (1990) 198–208.
[31] H. Li, A.M. Pajor, Mutagenesis of the N-glycosylation site of hNaSi-1 reduces transport activity, Am. J. Physiol. Cell. Physiol. 285 (2003) C1188–C1196.
[32] Y. Kanan, M.R. Al-Ubaidi, Role of tyrosine-sulfated proteins in retinal structure and function, Exp. Eye Res. 133 (2015) 126–131.
[33] N. Maeda, M. Ishii, K. Nishimura, K. Kamimura, Functions of chondroitin sulfate and heparan sulfate in the developing brain, Neurochem. Res. 36 (2011) 1228–1240.
[34] S. Lee, J.P. Kesby, M.D. Muslim, S.E. Steane, D.W. Eyles, P.A. Dawson, D. Markovich, Hyperserotonaemia and reduced brain serotonin levels in NaS1 sulphate transporter null mice, Neuroreport 18 (2007) 1981–1985.
[35] K. Sagawa, B. Han, D.C. DuBois, H. Murer, R.R. Almon, M.E. Morris, Age- and growth hormone-induced alterations in renal sulfate transport, J. Pharmacol. Exp. Ther. 290 (1999) 1182–1187.
[36] C. Hou, L.J. Wykes, L.J. Hoffer, Urinary sulfur excretion and the nitrogen/sulfur balance ratio reveal nonprotein sulfur amino acid retention in piglets, J. Nutr. 133 (2003) 766–772.
[37] V.F. Price, D.J. Jollow, Effects of sulfur-amino acid-deficient diets on acetaminophen metabolism and hepatotoxicity in rats, Toxicol. Appl. Pharmacol. 101 (1989) 356–369.
[38] S.T. Smale, D. Baltimore, The "initiator" as a transcription control element, Cell 57 (1989) 103–113.